Journal of Thermal Analysis and Calorimetry, Vol. 80 (2005) 11–26

THE USE OF THERMO-XRD-ANALYSIS IN THE STUDY OF ORGANO-SMECTITE COMPLEXES
Robert Mackenzie memorial lecture

S. Yariv[*] *and I. Lapides*

Department of Inorganic and Analytical Chemistry, Hebrew University of Jerusalem, Jerusalem 91904, Israel

Thermo-XRD-analysis is applied to identify whether or not the adsorbed organic species penetrates into the interlayer space of the smectites mineral. In this technique an oriented smectite sample is gradually heated to temperatures above the irreversible dehydration of the clay, and after each thermal treatment is diffracted by X-ray at ambient conditions. In the thermal treatment of organo-clays, under air atmosphere at temperatures above 250ºC, the organic matter is in part oxidized and charcoal is formed from the organic carbon. In inert atmosphere e.g. under vacuum above 250ºC the organic matter is pyrolyzed and besides small molecules, charcoal is formed. If the adsorbed organic compound is located in the interlayer space, the charcoal is formed in that space, preventing the collapse of the clay. A basal spacing of above 1.12 nm suggests that during the adsorption the organic compound penetrated into the interlayer space. Thermo-XRD-analyses of montmorillonite complexes with anilines, fatty acids, alizarinate, protonated Congo red and of complexes of other smectites with acridine orange are described. To obtain information about spacings of the different tactoids that comprise the clay mixture, curve-fitting calculations on the X-ray diffractograms were adapted.

Keywords: *acridine orange, alizarin, anilines, Congo red, fatty acids, montmorillonite, organo-smectite complexes, thermal analysis, X-ray*

Organo-smectite complexes

Smectite is a name of a group of clay minerals having a layer structure [1]. The most significant properties of smectites are their ability to swell, to adsorb inorganic and organic compounds, to behave as cation exchangers and to some extent also as anion exchangers and to be dispersed in water, and after certain treatments also in organic liquids.

Organo-smectite complexes are the products of the adsorption of organic compounds by smectites [2]. Different types of organic compounds – smectite associations are illustrated in Fig. 1. Organic cations are mainly adsorbed by a regular cation-exchange reaction, i.e. by replacing the inorganic cations initially present at the exchange sites, but a secondary adsorption of organic cations may occur by hydrophobic interactions [3, 4]. Secondary adsorption of cations, if occurs in excess, may change the charge of the clay layer from negative to positive. Organic polar molecules can be adsorbed due to polar interactions with polar sites inside the interlayer or on the smectite external surface. In the interlayers anhydrous or hydrated exchangeable metallic cations may serve as positive sites and the oxygen plane or water H-bonded to this plane, are the negative sites for polar interactions. On the external surface the broken bonds at the edges of the sheets, whether protonated or deprotonated, are the adsorption sites for polar molecules. The total charge of this surface depends on the acidity of the dispersing medium. Proton donors or acceptors are adsorbed due to the formation of H-bonds with appropriate sites inside the interlayers or on the smectite external surfaces. In the interlayers these are mainly water molecules, which belong to the hydration spheres of the exchangeable cations or are H-bonded to the O-planes, respectively. Organic anions are adsorbed mainly onto the external surface [2]. In the presence of exchangeable polyvalent metallic cations, anions may be adsorbed into the interlayer space due to short-range interactions of the basic anions with acidic metallic cations. Certain anions are adsorbed from aqueous solutions only if they are able to form stable positively charged coordination species [5, 6]. Organo-smectites in which the inorganic cations were replaced by organic large ammonium cations (e.g. quaternary ammonium cations) adsorb polar or non-polar organic molecules by secondary hydrophobic interactions [7].

The location of the adsorbed organic species, whether on the external surface of the clay crystal or inside the interlayer space, plays an important role on the properties of the organo-smectite complex. For ex-

* Author for correspondence: yarivs@vms.huji.ac.il

1388–6150/$20.00

Akadémiai Kiadó, Budapest, Hungary
Springer, Dordrecht, The Netherlands

ample, adsorption on the broken-bonds surface controls the colloidal behavior of the system [8–10]. Depending on the type of the organic compound and on the adsorbed amount, it may lead either to peptization or to flocculation of the clay. The interlayer space is peculiar in its surface acidity. It is rich with electron donation sites (the O-plane) as well as with Brønsted and Lewis acid sites (the hydrated and bare exchangeable cations). Smectites are therefore excellent catalysts for various reactions [11] and the interlayer space may change the chemical properties of the adsorbed molecules. Very often IR and visible absorption spectra of intercalated compounds are changed [9, 12, 13] as well as their thermal behavior [14].

In the 1940's the pioneers in the study of organo-smectites showed that organic cations may replace inorganic cations [15] and that the exchange capacity of small organic cations was similar to that of the inorganic Ba^{2+} [16]. They concluded that the adsorbed organic cations were located in the interlayers. Measurements on swelling are based on the XRD determinations of the *c*-axis spacing, obtained from the 001 reflection [17]. According to Fig. 1, when the organic species are adsorbed into the interlayer, they can lye either parallel to the clay layers (Fig. 1 – B_2) or tilted relative to the O-plane (Fig. 1 – B_1). The observations of Jordan [18] on the basal spacing of montmorillonite (Wyoming bentonite) treated with aliphatic amines of increasing chain length showed that up to amine with a chain of ten carbons a basal spacing of 1.36 nm is obtained. With longer chains, up to eighteen carbons, a spacing of 1.76 nm is obtained. Since the spacing of the collapsed clay is about 0.96 nm and the van der Waals thickness of the methyl group is 0.4 nm, he postulated that up to amines with a chain of ten carbons, the separation between the two silicate layers allows for the adsorbed organic amines to lye in zigzag flat along the clay surface, and to form a monomolecular layer. With chains of twelve to eighteen carbons, the separation between the two silicate layers allows for the adsorbed organic amines to form a bimolecular layer.

Robert Mackenzie was one of the pioneers in this field. He investigated the effect of water on the ethylene glycol-montmorillonite complexes [19] and showed the dependency of the basal spacing on the amount of adsorbed ethylene glycol and water. When the adsorbed glycol reaches 26%, a basal spacing of 1.71 nm is obtained with 4% water. With smaller amounts of water the basal spacing drops to 1.68 nm. When the adsorbed glycol is only 11.2 or 7.5%, basal spacings of 1.38 or 1.33 nm, respectively, are obtained with 4% water. But with increasing amounts of water, the basal spacing increases. He demonstrated that a basal spacing of 1.71 nm can be maintained by adding water if the glycol content is low, the additional water

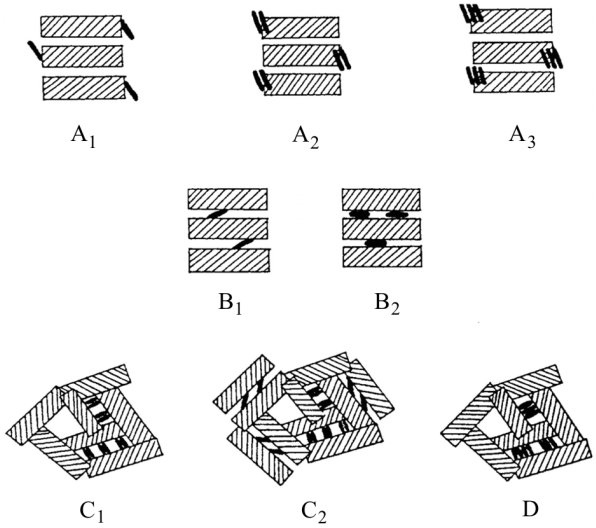

Fig. 1 Illustrations of the different types of organic compounds – smectite associations. A – adsorption onto the external surface of a tactoid; B – adsorption into the interlayer space of a tactoid; C and D – adsorption into the interparticle space of a floc [72]

being proportional to the glycol deficiency in the molecular ratio of about 6:1. According to the calculation mentioned above in connection with the adsorption of short and long chain aliphatic ammonium cations, basal spacings of 1.33–1.38 nm may indicate that the separation between the two silicate layers allows for the adsorbed ethylene glycol to lye in zigzag flat along the clay surface, and to form a monomolecular layer. Basal spacings of 1.68–1.71 nm may indicate that the separation between two silicate layers allows for the adsorbed molecules to form a bimolecular layer with glycol lying flat along the clay surface. It seems to us that the diffractograms, which were recorded after the adsorption of water, should be reexamined together with curve fitting calculations. It is possible that peaks, which characterize spacings of 1.43–1.64 nm are obtained from the tilting of the ethylene glycol-water association product, but it is also possible that overlapping of diffractograms of tactoids containing monomolecular layers with those of tactoids containing bimolecular layers are responsible for these observed spacings.

The basal spacings as determined from the XRD, not always can be conclusive on the penetration of the adsorbed organic molecule into the interlayer of the smectite. In Table 1 basal spacings of relatively small organic amine- and ammonium-complexes of montmorillonite (Wyoming bentonite) are gathered. The adsorption was carried out in 1% aqueous clay suspensions. Neat amines were added to the suspensions up to final concentrations of 0.10 mol L^{-1}. After 48 h samples were separated for XRD. Oriented samples were

Table 1 Basal spacings of Na-montmorillonite treated with organic amines (adsorbed amines) and of organic ammonium montmorillonites [19–25]

Adsorbed species	Basal spacing/nm	Adsorbed species	Basal spacing/nm
Organic amine molecules		Organic ammonium cations	
methylamine	1.26	methylammonium	1.26
trimethylamine	1.29	trimethylammonium	1.29
ethylamine	1.26	ethylammonium	1.27–1.28
diethylamine	1.30	diethylammonium	1.30–1.34
triethylamine	1.29	triethylammonium	1.32
tributylamine	1.35	tributylammonium	1.32
hexylamine	1.33	hexylammonium	1.32
ethylenediamine	1.34	ethylenediammonium	1.28–1.30
1,2-propylenediamine	1.34	1,2-propylenediammonium	1.30
1,3-propylenediamine	1.32	1,3-propylenediammonium	1.29
1,5-pentamethylenediamine	1.34	1,5-pentamethylenediammonium	1.30
diethylenetriamine	1.32	diethylenetriammonium	1.30–1.32
triethylenetetramine	1.34	triethylenetetrammonium	1.31–1.36
tetraethylenepentamine	1.34	tetraethylenepentammonium	1.32–1.34
benzylamine	1.52	benzylammonium	1.26
tribenzylamine	1.47	tribenzylammonium	1.25

obtained by air-drying on glass slides. The rest of the clay was washed six times with distilled water before preparing oriented samples for XRD. IR spectra showed that the unwashed samples contained mainly molecular amines whereas the washed samples contained only the protonated ammonium cations [20–25]. The table shows that the basal spacings range from 1.25 to 1.52 nm. These basal spacings do not supply an unequivocal proof for intercalation of the organic compounds, because the same spacings were obtained before the loading of the clay with amines due to the presence of interlayer water. A spacing of 1.23 nm characterizes Na-montmorillonite with a complete water monolayer, when the ratio between water molecules and the interlayer cation is 6 and 1.52 nm characterizes Na-montmorillonite with a complete water bilayer, when the ratio between water molecules and interlayer cation is 12 [26]. The claim of most investigators for intercalation of the organic compounds was based on the fact that in many of the studies the adsorbed amounts were high and the area of the external surface seemed to be too small to account for such high adsorptions. But we know today that the water content of the clay may also change if the organic matter is adsorbed only on the external surfaces.

A conclusive unequivocal proof from XRD data on the penetration of the adsorbed organic long chain amines into the interlayers was obtained by their adsorption onto vermiculite, an expanding clay mineral with surfaces having a high charge density [27]. In this case the long axis of the hydrophobic moiety was tilted with respect to the O-plane of the silicate layer. The angle of tilting increased with the increasing charge density of the clay layer. In these cases X-ray diffraction showed basal spacings higher than 2.0 nm, which increased with the length of the aliphatic chain. In the interaction of *n*-alkylammonium ions with vermiculite there is a 'keying in' of the ammonium groups in ditrigonal cavities. IR evidence indicates that N–H···O interactions exist but are weak. With the N–C bond normal to the silicate, and the alkyl chain in the ideal trans-trans configuration, the chain makes an angle of 54°44' with the silicate layer plane. Bi-ionic layer complexes of vermiculite have been observed by XRD at high solute concentrations. In the bilayer complex the two layers are accommodated back-to-back, so that their hydrophobic tails are buried in the interlayer space interior and their hydrophilic heads constitute the top and bottom of the space [28].

Thermo-XRD-analysis

Following the recommendation of ICTAC (International Confederation for Thermal Analysis and Calorimetry [29]) the definition of the various techniques comprising thermal analysis is as follows: 'Thermal analysis is a group of techniques in which a property of the sample is monitored *vs*. time or temperature while the temperature of the sample, in a specified atmosphere, is programmed. The program may involve heating or cooling at a fixed rate of temperature

change, or holding the temperature constant, or any sequences of these'. In thermo-XRD-analysis the sample is gradually heated to different temperatures and is diffracted by X-ray after each thermal treatment. This technique supplies information about the effect of temperature on different crystallographic features of solid particles.

Tactoids or oriented aggregates are clusters of parallel layers held by face-to-face interactions (FF associations). In smectite tactoids water layers of small thickness (less than 1.0 nm) separate the silicate layers. These layers comprise the interlayer space of the mineral [30]. According to Bragg's law, particles obtained from FF associations of similar layers, and have similar interlayer spaces, may diffract X-ray. Originally the term 'tactoids' was used to describe particles in colloid solutions and suspensions. In our publications it is also used for solid particles capable to diffract X-rays in powder mixtures.

Since 2004, to obtain information about the different tactoids that comprise the clay mixture, we adapted curve-fitting calculations on the X-ray diffractograms. If the powdered clay mixtures used for the X-ray diffraction are homogeneous, than sharp X-ray peaks are recorded with integral series of high order reflections. But it is not very often that the clay mixture is homogeneous. If there are tactoids with different basal spacings, the X-ray diffraction peak is broad with no integral series of high order reflections. This broad peak is composed of several components, each describing the basal spacing of a group of similar tactoids and the recorded peak is an average of these components. Sometimes two or more separate peaks are recorded but more often a peak with shoulders is recorded. If the relative number of tactoids is small, the information about their basal spacing may be lost in non-fitted diffractograms. It may be concluded that without curve-fitting the reliability of the information supplied from the diffractograms is limited. If the adsorption is small, curve fitting of the diffractograms is essential for having reliable information.

The diffractions shown by powdered smectites can be placed in two categories. One class consists of 00l basal reflections, which vary with the swelling or emptying of the interlayer space due to the adsorption or desorption, respectively, of water or organic matter. The second class consists of general diffractions, which are characteristic of the structure of the smectite layers themselves and are not dependent on the swelling of the clay. These are *hk* reflections, which in general are similar for all smectites. In the thermo-XRD-analysis of organo-smectites we are mainly interested in the 00l basal reflections. These patterns are obtained by mounting specimen of oriented smectite aggregates in front of the X-ray beam.

Thermo-XRD-analysis of natural smectites was used to prove that adsorbed water is located in the interlayer space [17]. Basal spacing recorded before the dehydration stage characterizes the hydrated state of the interlayer. This spacing, the diffuseness of the reflections, and the number of orders shown, vary from sample to sample depending on the thickness of the water layers and their regularity, which factors in turn are dependent on the exchangeable cation present and the water-vapor pressure, under which the sample has been equilibrated [31]. Usually it is in the range of 1.2–1.6 nm.

There is a large loss of water around 100°C, due to the removal of interlamellar water [17]. Corresponding to this, there is a collapse of the clay and the basal spacing shifts to shorter spacings, the exact value depending on the nature of the interlamellar cations. Up to 200°C, this dehydration is reversible and on bringing the dried smectite into contact with water, it will swell. Between 200 and 300°C the collapse tends to become irreversible. The exact temperature, at which this irreversibility is shown, depends on the type of smectite, on the dehydration energy of the exchangeable cations and on the size of the bare cations. Irreversible dehydration and collapse of dioctahedral smectites occur at temperatures lower than those of trioctahedral smectites. K- and Na-montmorillonite show it already at 200 and 300°C, respectively [17]. Di- and trivalent cations show it at higher temperatures. Li-montmorillonite loses its power to re-expand with moisture after heating in the range of 105–125°C due to the migration of Li on heating to the vacant octahedral sites [32].

The basal spacing usually decreases slightly on further heating up to about 500°C. The spacing of a full-collapsed smectite should be 0.94 nm [17]. However, for a full-collapse the interlamellar cations should cross the ditrigonal cavities of the O-planes into the tetrahedral sheet of the clay layer. 'Keying' of cations and anions in the ditrigonal cavities has been recently discussed [33]. The diameter of the ditrigonal cavity is about 0.3 nm. When the diameter of a bare interlayer cation is larger than that of the ditrigonal cavity, the collapse is disturbed and spacings higher than 0.94 nm are recorded. For example, Na-, Mg-, Cu- and Al-montmorillonite, when heated 3 h at 360°C, showed spacings of 0.96 nm with integral series of reflections. The diameters of these cations when they are bare of hydration are less than 0.3 nm. Cs- and Fe-montmorillonite showed spacings of 1.18 and 1.25 nm, respectively. The diameter of Cs cation is 0.334 nm, more than that of the ditrigonal cavity, whereas the dehydration of trivalent Fe requires a high energy. After heating the samples 3 h at 420°C, except for Cs, they all showed a spacing of 0.96 nm with integral series of reflections. Cs-mont-

morillonite showed a spacing of 0.99 nm, with no integral reflections [34].

Effect of temperature on the X-ray diffractions of unloaded montmorillonite

Montmorillonite (Wyoming bentonite) was heated at different temperatures and immediately, after each thermal treatment was diffracted by X-ray at ambient room temperature. The diffractograms were compatible with a gradual water loss. Figure 2 shows a curve fitted diffractogram of the sample heated at 420°C. The fitting indicated the presence of three components, with maxima at 0.95 (very strong), 0.98 nm (medium) and 1.07 nm (weak and very broad) with widths at half height of 0.38, 0.60 and 1.03 2θ, respectively. Each peak component represents a group of tactoids having the same basal spacing, which is determined from the 2θ of its maximum. Its width represents the homogeneity of this group. A sharp component is obtained when the group is highly homogeneous and the tactoids are very similar. The maxima of the two first components, labeled A_1 and A_2, characterize the presence of two types of tactoids of dehydrated collapsed montmorillonite. The appearance of these two varieties may be due to the fact that the Wyoming bentonite contains some exchangeable Ca, Mg and K in addition to the principal exchangeable Na. However, this must be further investigated.

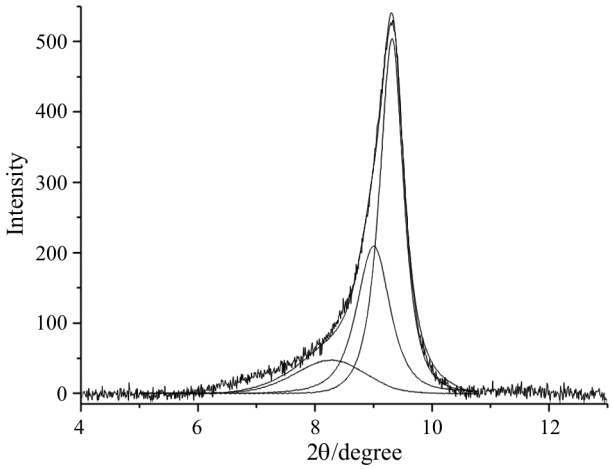

Fig. 2 Curve-fitted X-ray diffractogram of natural montmorillonite after thermal treatment at 420ºC

The third component labeled B, with a maximum at 1.07 nm, has a relatively small area and is very broad. A basal spacing in this range is too high to be attributed to a collapsed interlayer of Na-montmorillonite and too short to characterize interlayers with one water-monolayer, organic matter or charcoal. According to MacEwan [17] the thermal collapse of smectites with large exchangeable cations, which are not able to penetrate completely into the ditrigonal cavities, may give rise to such basal spacings. According to Marshall [35] hydroxyl anions are obtained in the interlayer as a result of hydrolysis of hydrated exchangeable cations. This kind of hydrolysis and the appearance of interlayer hydroxy- or oxy-groups coordinated to the exchangeable cations, become more significant with the thermal dehydration of montmorillonite (thermal hydrolysis). Russell and Fraser [36] demonstrated that at low levels of hydration protons migrate towards incompletely neutralized OH groups coordinated to Mg and Al in the octahedral sheet. It is supposed that this peak component characterizes tactoids with basal spacings of interlayers containing hydroxy- or oxy-cations, preventing complete collapse.

Indirect proofs for the intercalation of amines into montmorillonite

It was stated above that the basal spacings, which were determined by XRD, in most cases could not serve as a conclusive proof for the penetration of the adsorbed organic molecules into the interlayer of the substrate smectite. However, for many purposes it is very important to know whether the adsorbed organic compound has been intercalated. Here we describe a study in which the penetration of the adsorbed organic molecule into the interlayer has been proven indirectly. Bodenheimer *et al*. studied the adsorption of di- and polyamines by montmorillonite previously saturated with transition metal cations [19–25]. The formation of ligand-metal *d*-coordination complexes was identified from the deep staining of the clay. Since most of the exchangeable metallic cations were interlamellar, the investigators assumed that the adsorbed amines intercalated. Basal spacings of unloaded Cu- and Ni-montmorillonite and of montmorillonite loaded by Cu- and Ni-*d*-coordination complexes with ethylenediamine (En), all samples being air-dried, are gathered in Table 2. Similar results were obtained with other di- and polyamines (not shown in the table).

Heller-Kallai and Yariv [37] studied the swelling by steam of montmorillonite containing coordination *d*-complexes of transition metal cations with En. In Table 2 the effect of steam treatment on the basal spacings of Cu- and Ni-montmorillonite unloaded and loaded with different amounts of En, are gathered. The basal spacings obtained for air-dried samples did not supply evidence for the penetration of En into the interlayer. On the other hand the spacings recorded during steam treatment showed dependency on the loading. That is, with increasing amounts of En the expansion of the interlayer space by the penetration of water vapor became limited. In case of Ni-montmoril-

Table 2 Effect of steam on basal spacings of Cu- and Ni-montmorillonite containing ethylenediamine (En) [37]

Cation	En:cation molar ratio	Basal spacing/nm air-dried	Basal spacing/nm under steam
Cu^{2+}	0.0	1.22	1.90
$[Cu(En)]^{2+}+Cu^{2+}$	0.3	1.23	1.88, 1.64
$[Cu(En)]^{2+}+Cu^{2+}$	0.8	1.28	1.30–1.47
$[Cu(En)]^{2+}$	1.0	1.28	1.28
$[CU(En)_2]^{2+}+[Cu(En)]^{2+}$	1.6	1.27	1.28
$[Cu(En)_2]^{2+}+En$	2.6	1.27	1.28
Ni^{2+}	0.0	1.48	1.90
$[Ni(En)]^{2+}+Ni^{2+}$	0.5	1.38	1.84, 1.63
$[Ni(En)_2]^{2+}+[Ni(En)]^{2+}$	1.6	1.28	1.52
$[Ni(En)_2]^{2+}$	2.0	1.28	1.45
$[Ni(En)_3]^{2+}+[Ni(En)_2]^{2+}$	2.4	1.28	1.40
$[Ni(En)_3]^{2+}+En$	4.0	1.39	1.42

lonite the swelling by steam was not available after the formation of the complex $[Ni(En)_3]^{2+}$ inside the interlayer. In case of Cu-montmorillonite the swelling by steam was not available already with the formation of the complex $[Cu(En)]^{2+}$ inside the interlayer. This observation can be understood only if we assume that En has intercalated and ligand-metal *d*-complexes have been formed inside the interlayer space.

The adsorption of aniline and its derivatives by montmorillonite

In the period 1966–1973 our laboratory was involved in the study of the adsorption of aniline, its derivatives and other aromatic amines by different montmorillonites [38–43]. The principal research tool in this investigation was thermo-IR-spectroscopy. In this technique the organo-clay complex is gradually heated and at different temperatures its IR spectrum is recorded. We identified the bonds between the NH_2 group of the anilines and water molecules, which were hydrating the exchangeable cations, and after the dehydration of the clay, the bonds between the NH_2 group and the exchangeable metallic cations. Based on these observations we speculated that the anilines were intercalated.

Our goal was to reach a direct X-ray evidence for these intercalations. For this purpose we started to employ thermo-XRD-analysis. In our first thermal analysis [38] unloaded very thin clay films were heated up to 120°C under vacuum for half an hour. In most films under this thermal treatment the basal spacings dropped to less than 1.0 nm (Table 3), indicating their collapse. Cs-, Ca-, Co- and Ni-montmorillonite did not collapse under this thermal treatment and only part of the Cr-montmorillonite collapsed. The collapsed films were immersed in liquid aniline. It is obvious that any re-expansion of the collapsed clay resulted from its intercalation by aniline molecules. The expansion is shown in Table 3. The dehydrated collapsed Mg- and Zn-montmorillonite adsorbed aniline into their interlayer space, indicating that under the present thermal treatment their collapse was reversible. Tactoids of dehydrated collapsed K-, Mn- and Cd-montmorillonite did not swell in liquid aniline, indicating that under the thermal treatment these films have reached the stage of irreversible collapse. In the case of Li-, Na- and Al-montmorillonite, only part of the collapsed tactoids re-swell in contact with liquid aniline, indicating that only some of the tactoids which comprise these films, reached the stage of an irreversible collapse.

In the first years of our thermo-XRD-analyses of organo-smectites the clay films were heated in a vacuum furnace at 100–120°C. In Table 4 the basal spacings of air-dried films of monoionic montmorillonites, spacings of these films after they have been immersed for 48 h in liquid aniline derivatives and after heating the immersed films during 15 min at 100°C under vacuum are shown. The immersion of the films in the liquid anilines resulted in increase of the basal spacings, probably due to the penetration of the anilines into the interlayers. There was a decrease in spacing due to the thermal treatment. Before heating, some aromatic amines were present in molecular form, not coordinated to the transition metal cations but held in the interlayers by van der Waals forces. These were lost on heating and consequently the basal spacings dropped.

From the thermo-IR-spectroscopy analysis of the montmorillonite complexes with the anilines mentioned in Table 4 [41] three different associations between aniline, the inorganic cation and water molecules coordinating the cation were deduced (Fig. 3), labeled A, C and D. In association A direct metal-aniline coordination occurs in which the aniline-nitrogen donates an electron pair to the metallic cation. Consequently the proton donation ability of the NH_2 group increases relative to this ability of free aniline. In associations C and D a water molecule bridges between the metallic cation and the aniline. In C the nitrogen of ani-

Table 3 Basal spacings (in nm) of montmorillonites A – air dried films, unloaded and immersed 15 min in aniline liquid; B – films dried under vacuum at 120°C, unloaded and immersed 15 min in aniline liquid [38]

Interlayer cation	Basal spacings/nm			
	A. Air-dried		B. Dried under vacuum at 120°C	
	Unloaded	Immersed 15 min in aniline	Unloaded	Immersed 15 min in aniline
H^+	1.32	1.52	nd	nd
Li^+	1.28	1.53	1.00	1.48s, 1.00w
Na^+	1.47	1.55	0.98	1.49s, 1.00w
K^+	1.20	1.48	0.98	1.00
Cs^+	1.24	1.52	1.20	1.47
NH_4^+	1.22	1.55	1.00	1.40
Mg^{2+}	1.44	1.53	0.96	1.47
Ca^{2+}	1.49	1.55	1.17	1.50
Mn^{2+}	1.49	1.53	0.95	0.96
Co^{2+}	1.49	1.52	1.17	1.52
Ni^{2+}	1.48	1.52	1.17	1.52
Cu^{2+}	1.22	1.51	nd	nd
Zn^{2+}	1.39	1.53	0.96	1.49
Cd^{2+}	1.43	1.53	0.95	0.98
Al^{3+}	1.35	1.55	0.98	1.49w, 1.00s
Cr^{3+}	1.45	1.53	1.00d	1.53

s – a strong XRD peak; w – a weak XRD peak; d – a diffuse XRD peak; nd – not determined

Table 4 Basal spacings (in nm) of air-dried films of monoionic montmorillonites (I), of montmorillonite films immersed for 48 h in liquid aniline derivatives (II) and after heating the immersed films during 15 min at 100°C under vacuum (III) and the relative distribution of structures A, C and D in the interlayer space, determined from IR spectra [41]

Amine		Exchangeable cations				
		Mn^{2+}	Co^{2+}	Ni^{2+}	Zn^{2+}	Cd^{2+}
unloaded clay	I	1.49	1.48	1.48	1.39	1.43
aniline	II	1.50	1.50	1.51	1.51	1.51
	III	1.50	1.47	1.47	1.49	1.50
distribution of structures		$A^{++}C^{+++}$	$A^{++}C^{+++}$	$A^{+++}C^{++}$	$A^{++}C^{+++}$	$A^{++++}C^{+}$
o-toluidine	II	1.62	1.64	1.60	1.63	1.63
	III	1.58	1.62	1.52	1.59	1.63
distribution of structures		D^{+++++}	D^{+++++}	$C^{++++}D^{+}$	$A^{++}C^{+++}$	$A^{+++}C^{++}$
m-toluidine	II	1.67	1.63	1.58	1.67	1.59
	III	1.52	1.45	1.46	1.47	1.52
distribution of structures		$C^{++++}D^{+}$	$A^{+}C^{++++}$	$A^{++++}C^{+}$	$A^{+++}C^{++}$	$A^{++++}C^{+}$
2,5-dimethylaniline	II	1.72	1.77	1.71	1.71	1.72
	III	1.59	1.61	1.58	1.60	1.55
distribution of structures		D^{+++++}	D^{+++++}	D^{+++++}	$A^{++}D^{+++}$	$A^{++++}C^{+}$
2,6-dimethylaniline	II	1.65	1.63	1.65	1.65	1.65
	III	1.62	1.63	1.61	1.62	1.62
distribution of structures		D^{+++++}	D^{+++++}	D^{+++++}	D^{+++++}	$A^{+++}C^{++}$

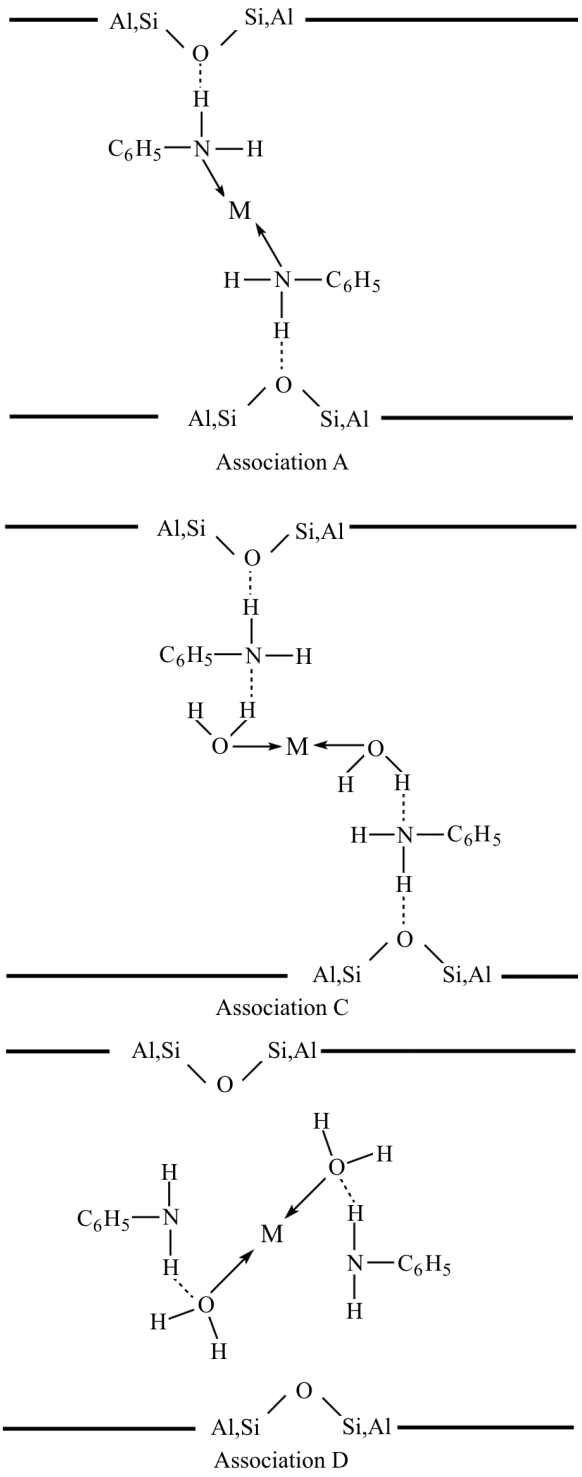

Fig. 3 Schematic presentations of associations A, C and D

line donates an electron pair to one of the protons of the bridging water molecule. In D the nitrogen of the aniline accepts one of the protons of this bridging water molecule. In association C the proton donation ability of the NH_2 group increases relative to this ability of free aniline, but in D the proton donation ability decreases. The relative distributions of structures A, C and D in the interlayer space, determined from IR spectra are shown in Table 4.

Except for Cd-montmorillonite, Table 4 shows a relatively good correlation between basal spacings and the dominant type of association formed in the interlayer space. Spacings of 1.45–1.55 nm are characteristic for tactoids intercalated by associations A and C. Spacings of 1.58–1.63 nm are characteristic for tactoids intercalated by associations D. In general the basal spacings of montmorillonites intercalated by associations A and C, with high proton donation abilities, are shorter than spacings of montmorillonites intercalated by association D, with low proton donation abilities. This is probably due to the formation of strong H-bonds with oxygens of the O-plane of the clay framework, and thus shortening the distance between the adsorbed molecules and the O-planes.

The adsorption of fatty acids by monoionic montmorillonites

In the 1970's the thermal treatment of the clay films in the vacuum furnace during the thermo-XRD-analysis was raised to 200°C. Thermo-IR-spectroscopy analysis showed that under this thermal condition the adsorbed organic compounds were only slightly decomposed, thus the results of the thermo-XRD-analyses appeared to be reliable. After this thermal treatment most films of unloaded montmorillonites showed a collapse and basal spacings of about 1.00 nm were obtained. We describe here one study in which this thermal treatment was applied simultaneously with thermo-IR-spectroscopy, the adsorption of the three fatty acids acetic, lauric and stearic by films of monoionic montmorillonites [45]. Immersing the films in the CCl_4 solutions resulted in the adsorption of the acids. Two distinct species were identified by IR spectroscopy in the clay phase, the carboxylic acid (RCOOH) and the carboxylate anion ($RCOO^-$). The latter is obtained by the deprotonation of the former after being adsorbed. The ratio between intensities of $RCOO^-$ IR band and RCOOH IR band gives qualitative information on the ratio between the anion and the acid.

The effect of the exchangeable cations on this ratio is shown in Table 5. The ratios of the two adsorbed species were found to be dependent both on the nature of the exchangeable cation and on the chain length of the acid. Surprisingly, in Al- and Fe-montmorillonite, in which the surface acidity is expected to be high [46], the anionic species predominate, whereas in Cs-montmorillonite, in which the surface basicity is expected to be high, the acidic species predominate.

Basal spacings, which were determined during the thermo-XRD-analysis of the films, are shown in

Table 5. The immersion of the films in the CCl_4 solutions of the different acids did not show a significant increase in the basal spacings, which might indicate the penetration of the acids into the interlayers. There was a decrease in spacing due to the thermal treatment. Before heating some of the acids were present in molecular form, not coordinated to the transition metal cations but held in the interlayers by van der Waals forces. These, together with water molecules, were lost on heating at 200°C under vacuum and consequently the basal spacings decreased. After this thermal treatment all the samples showed basal spacings higher than those obtained with the unloaded films heated at 200°C under vacuum, suggesting that adsorbed acids were located inside the interlayers.

When this study was submitted for publication, the paper was sent to Robert Mackenzie for reviewing. In his report he wrote that he was pleased to see a paper demonstrating the unique nature of the interlayer space of montmorillonite in leading to the dissociation of the fatty acids. The thermo-XRD-analysis proved that the peculiar behavior of the three acids occurred inside the two-dimensional space between the lamellae.

The role of interlamellar charcoal in the thermo-XRD-analysis of organo-smectites

In the 1980's there was a great progress in the understandings of the exothermic reactions, which are responsible for the exothermic peaks in the DTA curves of organo-clay complexes recorded in air. DTA-TG studies were supplemented by evolved gas analysis (EGA). The evolved gases were examined by mass spectrometry simultaneously with the DTA runs [47–53]. Based on most of the publications of DTA curves of organo-clays since the forties, the following was concluded on the DTA runs of organo-smectites [14, 54, 55]. When they are carried out in air atmosphere, at about 250°C the oxidation of the adsorbed organic matter begins. In the case that the DTA runs are carried out under nitrogen or argon this is also the temperature at which pyrolysis of the adsorbed organic matter begins. Three steps of oxidation and two or three steps of pyrolysis for DTA runs in air or under inert atmosphere, respectively, were identified. In air, the first oxidation step occurs in the temperature range 250–500°C. At this stage the organic H atoms are combined with air oxygen atoms to form water. Because of the limited amount of oxygen in air, relative to the amount of the adsorbed organic matter, only part of the organic C and N atoms are oxidized to form CO_2 and NO_2 molecules [56–58]. EGA study of dye-smectites confirmed that more moles of H_2O than CO_2 and NO_2 were evolved at this temperature [51, 54, 59]. The rest of C and N atoms form a black residue, termed by some investigators as 'petroleum coke' and by other as 'charcoal'. In the second and third steps of the oxidation (sometimes referred as the second step a and the second step b) in the temperature ranges 400–600 and 550–800°C, respectively, charcoal is oxidized to CO_2 and NO_2. DTA curves of natural resins showed similar oxidation steps [60]. In inert atmosphere the pyrolysis products are mainly H_2, CH_4 and NH_3 in addition to charcoal obtained by the condensation of the residual organic matter. A high temperatures evolution

Table 5 Columns a – X-ray diffractions: Basal spacings (nm) of monoionic montmorillonites unloaded and loaded by acetic, lauric and stearic acids. Samples were diffracted after five days equilibration at 40% humidity (room temperature) and after heating the samples under vacuum at 200°C during 15 min. Columns b – Infrared spectra: Effects of exchangeable cations on the ratios between intensities of $RCOO^-$ IR bands and of RCOOH IR bands [45]

Exchangeable cations	Treatment	Unloaded	Loaded by					
			acetic acid		lauric acid		stearic acid	
		a	a	b	a	b	a	b
H^+	*r.t.*	1.46	1.47	0.5	1.46	0.3	1.45	0.2
	heated	0.99	1.29		1.39		1.37	
Na^+	*r.t.*	1.23	1.21	0.4	1.30	1.3	1.28	1.1
	heated	0.97	1.23		1.26		1.20	
Cs^+	*r.t.*	1.23	1.25	0.3	1.25	0.3	1.27	0.3
	heated	1.12	1.24		1.18		1.22	
Ca^{2+}	*r.t.*	1.54	1.51	0.3	1.52	0.6	1.52	0.6
	heated	0.99	1.44		1.48		1.46	
Al^{3+}	*r.t.*	1.52	1.55	1.2	1.50	1.2	1.47	1.6
	heated	1.14	1.38		1.37		1.36	
Fe^{3+}	*r.t.*	1.39	1.45	2.0	1.50	0.7	1.40	0.8
	heated	0.98	1.25		1.38		1.32	

Basal spacing (nm); ratios between intensities of $RCOO^-$ band and of RCOOH band in IR spectra of the samples

of the adsorbed non-decomposed organic compound was also identified in several cases.

There seems to be several types of charcoal, which are formed simultaneously during the thermal analysis of the organo-clays, responsible for the appearance of exothermic peaks at different temperatures during the DTA runs. Not very much is known on the fine structure of the charcoal-clay complexes. The assumption on the presence of several types of charcoal is based on the fact that the oxidation of charcoal occurs in steps. In other words, the different charcoals are combusted at different temperatures giving rise to different exothermic peaks in the DTA curves.

Several factors were identified to control the type of charcoal formed during the thermal treatment. For example, the features of the charcoal depend very much on the nature of the precursor adsorbed organic species. Consequently, each ammonium montmorillonite has its characteristic DTA exothermic peak temperatures [54, 55]. Charcoal formed in an interlayer space is stable to higher temperatures than charcoal formed on the external surface of the clay mineral. Consequently, the last exothermic peak in the DTA of organo-smectites occurs at higher temperatures than the last exothermic peak of organo-kaolinite or illite. A combined DTA-EGA study of smectites loaded by different aromatic cationic dyes (40–50 mmol dye per 100 g clay) showed that in montmorillonite the last oxidation stage and the evolution of CO_2 occurs at higher temperatures than in laponite suggesting that the thermal stability of the montmorillonite-charcoal should be higher [51].

Yermiyahu *et al*. [34] identified by the thermo-XRD-analysis of several monoionic montmorillonites loaded with the anionic azo dye Congo red, two types of charcoal, giving rise to spacings of 1.10–1.33 and of 1.61–2.19 nm. Since the van der Waals diameter of carbon atom is 0.34 nm, the former should be composed of monolayers of carbon atoms. Basal spacings smaller than 1.2 nm may indicate that atoms of the monolayer carbon charcoal are 'keying' into the hexagonal holes of the oxygen plane. The latter may be a multilayer carbon or composed of fragments of hexagonal carbon layers, lying in the interlayer space in a disorder, tilted relative to the oxygen plane. The different types of charcoal-montmorillonite complexes were formed in one organo-clay sample. Since the different complexes diffracted the X-ray radiation, it is assumed that the clay powder contains homogeneous tactoids with the different basal spacing and that each tactoids is responsible for certain diffraction. The rise in temperature from 360 to 420°C leads to the rearrangement of some of the monolayer carbon charcoal into multilayer carbon charcoal probably from thermal condensation of small monolayer carbon charcoal fragments.

In another study Yermiyahu *et al*. [61] identified by DTA two types of charcoal, a low and a high temperature stable charcoal. From the shapes of the DTA curves of monoionic montmorillonites saturated with different exchangeable metallic cations and loaded by the anionic dye Congo red, and from the area of the different exothermic peaks, they concluded that the surface acidity controls the type of charcoal, which is formed in the interlayer. A high surface acidity favors the formation of a high temperature stable charcoal whereas a low surface acidity favors the formation of a low temperature stable charcoal.

Carbonization of organic matter in the interlayer space of montmorillonite was investigated by the graphitizing of polymers between the lamellae by Sonobe *et al*. [62–65]. The black residue obtained at 700°C was a film shape highly stacked structure with small interplanar spacing of 0.337 nm. The formation of such a unique coke is attributed to the peculiar carbonization method where the two-dimensional space between the lamellae serves as a unique field for carbonization. In the 1990's, when the idea on the formation of charcoal in the interlayer space of smectites by thermal treatment was established, we decided to use its formation as a direct proof for the intercalation of the precursor adsorbed organic species. For this purpose analyzed samples were heated up to 300, 360 and recently, also up to 420°C.

In some cases the interlamellar organic compound is evolved during heating before the formation of charcoal. In these cases the diffractograms recorded after 300°C show a spacing of about 1.0 nm characteristic for collapsed tactoids. Preliminary experiments in which the organo-smectite complexes were thermally treated in alkali halide matrices gave positive results. The escape of the adsorbed organic compound may depend on the bonding strength of the exchangeable cation with the adsorbed organic molecule. For example, in urea-montmorillonite complexes no charcoal was observed at 375°C in Li-, Na-, K-, Mn- and Cu-montmorillonite but was observed in H-, Rb-, Cs-, Mg-, Ca-, Al- and Fe-montmorillonite (paper in preparation).

Thermo-XRD-analysis of the adsorption of alizarinate by Na-, Al-, Co-, Ni- and Cu-montmorillonite

Fully protonated alizarin (Scheme 1) is insoluble in water but at pH between 6.8 and 10.1 it is soluble. At this environment the OH group attached to carbon 1 dissociates and alizarin is transformed to the red monovalent alizarinate anion. Divalent transition metal cations and Al^{3+} form stable six-member chelate ring complexes with this ligand through the deprotonated 1-hydroxyl oxygen and the adjacent car-

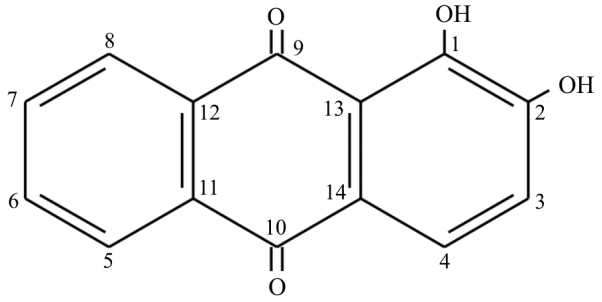

Scheme 1 Alizarin (1,2-dihydroxyanthraquinone)

bonyl oxygen [66, 67]. Na-, Co- and Ni-montmorillonite adsorbed in aqueous suspensions at pH 9 up to 4, 13 and 13 mmol alizarinate per 100 g clay, respectively, onto their broken-bonds surface whereas Al- and Cu-montmorillonite adsorbed up to 25 mmol dye per 100 g clay into their interlayer spaces.

Unloaded Na-, Al-, Co-, Ni- and Cu-clays and samples loaded with increasing amounts of alizarinate, were heated in air up to 360°C [9, 10]. After each thermal treatment they were diffracted by X-ray at room temperature. Representative thermo-XRD curves of Co- and Cu-montmorillonite unloaded and loaded with different amounts of alizarinate are shown in Fig. 4. Diffractograms of the unloaded and loaded non-heated Na-, Co-, Ni- and Cu-clays showed spacings of 1.22–1.24 nm, characterizing tactoids with interlamellar water or hydrated alizarinate monolayers and those of Al-montmorillonite showed basal spacings of 1.40–1.50 nm, characterizing interlamellar water or hydrated alizarinate bilayers. With the rise in temperature the basal spacings of all samples decreased. After heating at 360°C spacings of unloaded and alizarinate loaded Na-, Co- and Ni-montmorillonite were below 1.0 nm, characterizing collapsed montmorillonites, suggesting that initially the adsorbed alizarinate was not located in the interlayer. Spacings of unloaded Cu- and Al-montmorillonite, after heating at 360°C were also below 1.0 nm, but those of alizarinate loaded Cu- and Al-montmorillonite, after heating at this temperature were in the range 1.1–1.2 nm, and the samples became black, characterizing the presence of interlamellar charcoal, suggesting that initially in these clays the adsorbed alizarinate was located inside the interlayer space. Curve fitted diffractograms will be published in [68].

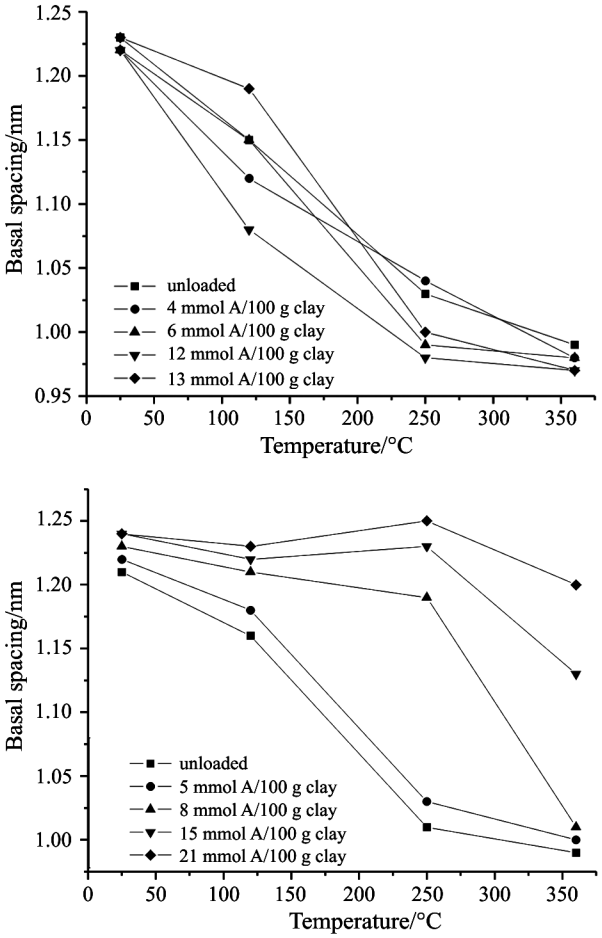

Fig. 4 The effect of temperature on the basal spacing of unloaded smectites and of smectites loaded with increasing amounts of alizarinate top – Co-montmorillonite; bottom – Cu-montmorillonite [10]

Thermo-XRD-analysis of montmorillonite treated with protonated Congo red. Curve fitting

As an example for the importance of curve fitting, the thermo-XRD-analysis of the adsorption of protonated Congo red (CR, Scheme 2) by montmorillonite is described [69]. CR is an anionic dye. At pH 1 four of the N atoms are protonated and it becomes cationic. At this pH it was adsorbed into the interlayer space of the clay by the mechanism of cation exchange. Samples were prepared with increasing amounts of protonated CR. To obtain films with preferred orientation, 1 mL of each aqueous suspension was air-dried on a glass slide. The samples were gradually heated to 420°C and diffracted at room temperature after each thermal treatment. Diffractograms of samples treated at 420°C showed broad peaks and were curve-fitted to determine the different components, which composed the XRD peaks. The broad peak of one sample may con-

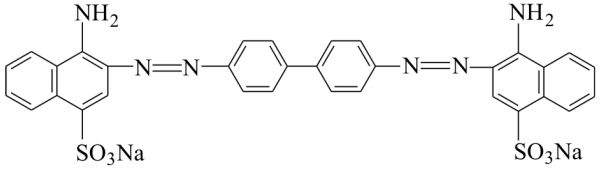

Scheme 2 Congo red (diphenyl-4,4'-bis-azo-2-naphthylamine-1-1-sulphonic acid-4)

tain up to four components. Characteristic features of curve-fitted X-ray diffractograms of samples thermally treated at 420°C are summarized in Table 6.

Component A, with a maximum at 0.95–0.98 nm, characterizes the presence of tactoids with collapsed interlayers. As one would expect there is a trend of the relative area of this component to decrease with the loading of the clay. This component is very sharp in the diffractograms of the unloaded clay (0.38 2θ) but becomes broader after the loading (0.70±0.08 2θ), indicating that this group of tactoids becomes less homogeneous due to the loading. Component B at 1.05–1.07 nm characterizes tactoids with a non-complete collapse, probably due to the presence of interlamellar hydroxy- or oxy-cations. The width of this component (1.05 ±0.02 2θ) and its relative area (25±4%) are not affected by the loading. Component C at 1.22–1.31 nm characterizes tactoids with intercalated planar monolayers of charcoal. As one would expect there is a trend of the relative area of this component to increase with the loading of the clay. Component D at >1.60 nm characterizes tactoids with expanded interlayers containing intercalated multilayer carbon charcoal. This peak component is very broad (width at half height >3.2 2θ) suggesting that this group of tactoids is inhomogeneous. In the presence of high amounts of adsorbed organic matter components A and B converge at 1.01 nm, and component C splits into two sub-components C_1 and C_2, with maxima at 1.12 and 1.27–1.31 nm, respectively. The former spacing represents intercalated monolayer carbon charcoal with atoms 'keying' into the ditrigonal holes of the O-plane. In the latter spacing the distance between the silicate layers allows for the monolayer carbon charcoal to lie in this space without the keying of carbon atoms into the ditrigonal cavities of the O-plane.

The presence of components C and D in the curve-fitted diffractograms of samples heated above 300°C suggests that before the thermal treatment the adsorbed protonated CR was located inside the interlayer space of the smectite. Depending on the amount of adsorbed CR, three types of diffractograms were identified. With small adsorption (7.5 and 22.5 mmol CR per 100 g clay) components A, B and C were identified. With higher adsorption (45.0 and 52.5 mmol CR per 100 g clay) components A, B, C and D were identified and with very high adsorption (67.5 and 75.0 mmol CR per 100 g clay), components A+B, C_1, C_2 and D were identified.

Determination of the surface basicity of smectites by acridine orange

Basicity of the O-planes which border the interlayers arises from the ability of oxygen atoms to donate non-bonding lone-pair electrons to acidic entities. The basic strength of the O-plane depends on whether there is an isomorphic tetrahedral substitution of Al for Si. The induction of tetrahedral Al on the non-bonding electrons of the O atoms is weaker than that of Si. Consequently the basic strength of the O-plane should increase with tetrahedral substitution [31, 44]. The basic strength of the O-plane also depends on whether the clay is di- or trioctahedral. In trioctahedral smectites, oxygen bridging between the tetrahedral and octahedral sheets, is coordinated by four atoms (one Si and three Mg) and has no contribution to $d\pi$–$p\pi$ bond with

Table 6 Characteristic features of curve-fitted X-ray diffractograms of thermally treated at 420°C natural montmorillonite and montmorillonite loaded with increasing amounts of protonated CR (peak component maxima in nm, relative peak areas in % of total peak area, and widths at half height in 2θ). All samples were diffracted at room temperature

Peak component		Curve fitting parameters	Loading (mmol CR/100 g clay)						
			0.0	7.5	22.5	45.0	52.5	67.5	75.0
A		location max/nm	0.95*, 0.98#	0.97	0.98	0.98	0.98	1.01+	1.01+
		width at $h_{0.5}$/2θ	0.38	0.64	0.70	0.77	0.69	1.15	0.90
		relative area/%	77	51	53	29	34	34	28
B		location max/nm	1.07	1.05	1.07	1.07	1.07		
		width at $h_{0.5}$/2θ	1.03	1.06	1.08	1.07	1.06		
		relative area/%	23	29	22	20	23		
C	C_1	location max/nm						1.12	1.12
		width at $h_{0.5}$/2θ						1.36	1.27
		relative area/%						30	35
	C_2	location max/nm		1.25	1.26	1.21	1.22	1.31	1.27
		width at $h_{0.5}$/2θ		2.25	2.72	1.72	1.64	1.55	1.95
		relative area/%		20	25	45	37	18	30
D		location max/nm				1.86	1.64	1.68	1.81
		width at $h_{0.5}$/2θ				3.96	3.18	3.30	3.52
		relative area/%				6	6	18	7

*a very strong peak component A_1; #a medium size peak component A_2; +peak components A+B.

the Si. On the other hand, in dioctahedral clays, the bridging oxygen is coordinated by three atoms, (one Si and two Al) and it has a small contribution of a lone electron pair to $d\pi$–$p\pi$ bond with the Si. Consequently the contribution of atoms of the O-plane to the π system of Si decreases, and the electron density at the non-bonding orbitals of the oxygens becomes high, compared to their density at non-bonding orbitals of trioctahedral clays. Thus the basic strength of the O-plane of dioctahedral clays, although weak, should be higher than that of trioctahedral clays [13].

The surface basicity of the O-planes of Na-beidellite, Na-montmorillonite, Na-saponite and Na-laponite was studied by visible spectroscopy of clay suspensions loaded with the metachromic cationic dye acridine orange (AO, Scheme 3) [70–74]. Metachromasy of AO in aqueous solutions can be described by the effect of concentration on the absorption spectrum. The absorption spectrum of very dilute AO solutions shows a maximum at 492 nm and a shoulder at 470 nm, labeled bands α and β, respectively. More concentrated dye solutions demonstrate metachromasy, i.e. the intensity of band β becomes higher than that of band α. A further increase in concentration results in the displacement of band β to wavelengths below 470 nm while band α remains at 492 nm. The appearance of band β at 470 nm is due to the dimerization of AO. Two parallel dye cations are held together by the interaction between their π electrons. The shift of band β from 470 to lower wavelengths indicates trimerization and tetramerization of AO.

A metachromic band in the spectrum of AO adsorbed by smectite minerals is an indication of π interactions in which the π antibonding orbitals of the dye cations accept lone electron pairs from oxygen atoms of the O-plane of the clay. Curves describing the wavelength of the metachromic band β in the presence of the clay as a function of the degree of loading (photometric titration curves, Fig. 5), showed three regions. In the first region the clay is well peptized. The adsorbed cation is located inside the interlayer space (Fig. 1 – B_2). The location of band β depends on the smectite (Table 7) but it does not change through the whole first region. In this region the spectrum of AO in laponite suspensions does not show band β, indicating that there is no donation of electrons from the O-plane of laponite to the aromatic antibonding π orbitals of AO.

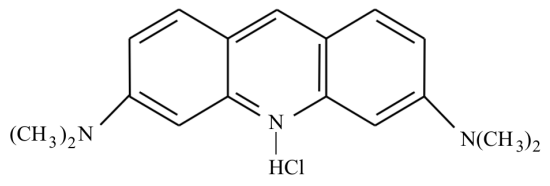

Scheme 3 Acridine orange [3,6-bis(dimethylamine)acridine hydrochloride]

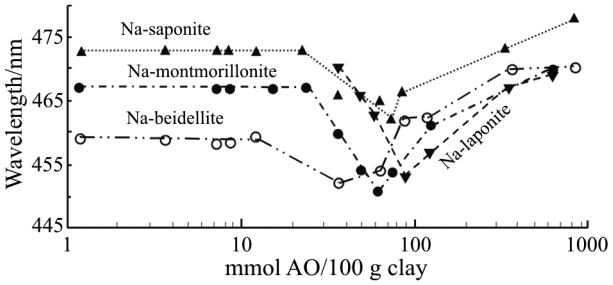

Fig. 5 Wavelength curves of aqueous suspensions of Na-smectites treated with different amounts of acridine orange. The wavelength (in nm) of band b is given *vs.* the total amount of dye in the suspension (in mmol) calculated per 100 g clay [71]

In the second region the clay flocculates and the maximum of band β shifts to lower wavelengths. At this stage dimmers and higher polymers are obtained in the interparticle space of the floc (Figs 1 – C and D and Table 7). In the third region the clay is repeptized and the maximum of band β shifts back to higher wavelengths. At this stage dye cations (monomers or dimmers) are adsorbed on the broken-bonds surface changing its charge from negative to positive, thus leading to peptization (Fig. 1 – A and Table 7). Rytwo and Ruiz–Hitzky measured adsorption enthalpies of the cationic dyes methylene blue and crystal violet by montmorillonite [75]. Although not stated by these authors, from their data it appears that calorimetric titrations of montmorillonite by these dyes show three regions.

The X-ray data of Table 7 show that except for saponite, during the thermal treatment at 300°C, the unloaded smectites collapsed and the basal spacing dropped to about 1.0 nm. Laponite required 4 days of heating under vacuum for this collapse. All loaded smectites under a similar thermal treatment became black and showed higher basal spacings, proving the presence of intercalated charcoal. The presence of interlamellar charcoal indicates that the adsorbed AO was located inside the interlayer.

The table also shows the spacings after dehydrating the clay films at 100°C under vacuum. Based on the fact that the van der Waals diameter of carbon is 0.34 nm, the spacing of ≈1.3 nm obtained in the first region of the photometric titration indicates that monomeric dye cations were located in the interlayer with the aromatic rings lying parallel to the smectite layers. In this region, π interactions between the O-plane of the clay and AO are possible. In the second and third regions, the spacing may account for a bilayer of AO and/or water. Tilting of the cationic dye relative to the silicate layer is also possible at this stage although the X-ray data cannot serve as conclusive evidence for this. Anyhow metachromasy at this stage may be due to the aggregation of the dye cations.

Table 7 Three regions in the wavelength curves of Fig. 5 (photometric titrations in mmol AO per 100 g clay), minimum wavelength of band β in the three regions (in nm) and basal spacings (in nm) obtained in the thermo-XRD-analysis [71]

Region of photometric titration	Loading in mmol AO per 100 g clay	Minimum wavelength of band β/nm	Basal spacings/nm		
			40% relative humidity	100°C under vacuum	300°C under vacuum
Na-beidellite					
unloaded			1.45, 1.30	1.22	1.00
1st region	0–15	458	1.43	1.27	1.26
2nd region	15–37	452	1.36	1.30, 1.62	1.27
3rd region	120*	>452	1.78	1.71	1.38
Na-montmorillonite					
unloaded			1.25	1.15	0.96
1st region	0–30	467	1.39	1.30	1.20
2nd region	30–62	451	1.60	1.57	1.32
3rd region	120*	>451	1.64	1.62	1.36
Na-saponite					
unloaded			1.26	1.26	1.26
1st region	0–25	473	1.37	1.34	1.31
2nd region	25–72	462	1.58, 1.35	1.51, 1.35	1.31
3rd region	120*	>462	1.64	1.60	1.34
Na-laponite					
unloaded			1.23	1.30	1.00**
1st region	0–15	no band β	1.33	1.28	1.14
2nd region	15–85	453	1.46	1.42	1.31
3rd region	120*	>453	1.59	1.56	1.31

*Sample used for X-ray study; **after 4 days thermal treatment under vacuum

From these data it is obvious that metachromasy, which was observed in the first region of the photometric titration of beidellite, montmorillonite and saponite resulted from π interactions between the organic cations and the O-plane. With increasing ability of the O-plane to donate electron pairs, the energy level of the unoccupied antibonding orbitals of AO is raised and the $\pi \rightarrow \pi^*$ transition of the adsorbed species shifts from 492 nm to lower wavelengths. In the first region the lowest wavelength of band β is obtained with beidellite. Longer wavelengths are obtained with montmorillonite and saponite whereas laponite does not show any metachromasy. It may therefore be concluded that the basic strength of the O-plane decreases in the order: beidellite, montmorillonite, saponite and laponite.

Conclusions

Basal spacings as determined from XRD of organo-smectite complexes, not always supply conclusive information on the penetration of the adsorbed molecules into the interlayers. If the adsorbed organic compound is not volatile, thermo-XRD-analysis can give an answer to this question. For example, at 360°C complexes of alizarinate with Na-, Co- and Ni-montmorillonite collapse, giving basal spacing of about 1.0 nm indicating that the adsorption of the organic anion took place on the external surface of the clay. On the other hand, during a similar thermal treatment of complexes of alizarinate with Cu- and Al-montmorillonite, charcoal is formed in the interlayer, preventing the collapse of the clay. A basal spacing of about 1.2 nm suggests that during the adsorption the anion penetrated into the interlayer. Thermal treatment under vacuum to lower temperatures in some cases can supply information on the arrangement of the organic compound inside the interlayer space. For example, smectites loaded by small amounts of acridine orange, after drying at 100°C gave spacings of ≈1.3 nm, suggesting that the dye cation was lying inside the interlayer space parallel to the silicate layer. This arrangement enables atoms of the O-plane to donate electron pairs to the antibonding π orbitals of the aromatic rings. Curve fitting calculations of diffractograms of protonated Congo red montmorillonite complexes heated at 420°C revealed the presence of three types of charcoal formed in the interlayers.

References

1 S. Yariv and K. H. Michaelian, in: S. Yariv and H. Cross (Eds) Organo-Clay Complexes and Interactions, Marcel Dekker, Inc., New York 2002, p. 1.
2 S. Yariv, in: S. Yariv and H. Cross (Eds) Organo-Clay Complexes and Interactions, Marcel Dekker, Inc., New York 2002, p. 39.
3 R. E. Grim, W. H. Allaway and F. L. Cuthbert, J. Amer. Ceram. Soc., 30 (1947) 137.
4 W. F. Bradley and R. E. Grim, J. Phys. Chem., 52 (1947) 1404.
5 S. Yariv, W. Bodenheimer and L. Heller, Israel J. Chem., 2 (1964) 201.
6 S. Shoval and S. Yariv, Clays Clay Minerals, 27 (1979) 29.
7 R. F. Giese and C. J. van Oss, in: S. Yariv and H. Cross (Eds) Organo-Clay Complexes and Interactions, Marcel Dekker, Inc., New York 2002, p. 175.
8 H. van Olphen, Clay Colloid Chemistry, Interscience, New York 1963, p. 160.
9 M. Epstein and S. Yariv, J. Colloid Interface Sci., 263 (2003) 377.
10 M. Epstein, I. Lapides and S. Yariv, Colloid Polym. Sci., 282 (2005) in press.
11 L. Heller-Kallai, in: S. Yariv and H. Cross (Eds) Organo-Clay Complexes and Interactions, Marcel Dekker, Inc., New York 2002, p. 567.
12 S. Yariv, in: S. Yariv and H. Cross (Eds) Organo-Clay Complexes and Interactions, Marcel Dekker, Inc., New York 2002, p. 345.
13 S. Yariv, in: S. Yariv and H. Cross (Eds) Organo-Clay Complexes and Interactions, Marcel Dekker, Inc., New York 2002, p. 463.
14 A. Langier-Kuźniarowa, in: S. Yariv and H. Cross (Eds) Organo-Clay Complexes and Interactions, Marcel Dekker, Inc., New York 2002, p. 273.
15 J. E. Gieseking, Soil Sci., 47 (1939) 1.
16 S. B. Hendricks, J. Phys. Chem., 45 (1941) 65.
17 D. M. C. MacEwan, in: G. W. Brindley (Ed.) X-ray Identification and Crystal Structures of Clay Minerals, The Mineralogical Society, London 1951, p. 86.
18 R. C. Mackenzie, Trans. Faraday Soc., 44 (1948) 368.
19 W. Bodenheimer, B. Kirson and S. Yariv, Israel J. Chem., 1 (1963) 69.
20 W. Bodenheimer, L. Heller, B. Kirson and S. Yariv, Clay Minerals Bull., 5 (1962) 145.
21 W. Bodenheimer, L. Heller, B. Kirson and S. Yariv: in I. Th. Rosenquist (Ed.) Proc. First Intern. Clay Conf., Stockholm, August 12–16, 1963, Pergamon Press, Oxford 1963, Vol. 2, p. 351.
22 W. Bodenheimer, L. Heller, B. Kirson and S. Yariv, Israel J. Chem., 1 (1963) 391.
23 W. Bodenheimer, L. Heller and S. Yariv, in: L. Heller and A. Weiss (Eds), Proc. Second Intern. Clay Conf., Jerusalem, June 20–26, 1966, Israel Program for Scientific Translations, Jerusalem 1966, Vol. 1, p. 251.
24 W. Bodenheimer, L. Heller and S. Yariv, in: L. Heller and A. Weiss (Eds), Proc. Second Intern. Clay Conf., Jerusalem 1966, Israel Program for Scientific Translations, Jerusalem 1966, Vol. 2, p. 171.
25 S. Yariv, Ph.D. Thesis (in Hebrew). Submitted to the Senate of the Hebrew University, Jerusalem 1964.
26 F. Kraehenbuehl, H. F. Stoeckli, F. Brunner, G. Kahr and M. Mueller-Vonmoos, Clay Minerals, 22 (1987) 1.
27 J. L. Perez-Rodriguez and C. Maqueda, in: S. Yariv and H. Cross (Eds) Organo-Clay Complexes and Interactions, Marcel Dekker, Inc., New York 2002, p. 113.
28 F. G. Walker, Clay Minerals, 7 (1967) 129.
29 J. O. Hill (Ed.), For Better Thermal Analysis and Calorimetry, 3rd Edition, International Confederation for Thermal Analysis, Bundoora, Australia 1991.
30 S. Yariv and H. Cross, Geochemistry of Colloid Systems, Springer Verlag, Berlin 1979, p. 199, 356 and 405.
31 S. Yariv, in: M. Schrader and G. I. Loeb (Eds) Modern Approach to Wettability, Plenum Press, New York 1992, p. 279.
32 U. Hofmann and R. Klemen, Z. anorg. Chemie, 262 (1950) 95.
33 S. Yariv, I. Lapides, K. H. Michaelian and N. Lahav, J. Therm. Anal. Cal., 56 (1999) 865.
34 Z. Yermiyahu, I. Lapides and S. Yariv, J. Therm. Anal. Cal., 69 (2002) 317.
35 C. E. Marshall, The Colloid Chemistry of the Silicate Minerals, Academic Press, Inc., New York 1949, p. 121.
36 J. D. Russell and A. R. Fraser, Clays Clay Minerals, 19 (1971) 55.
37 L. Heller-Kallai and S. Yariv, J. Colloid Interface Sci., 79 (1981) 479.
38 S. Yariv, L. Heller, Z. Sofer and W. Bodenheimer, Israel J. Chem., 6 (1968) 741.
39 Z. Sofer, L. Heller and S. Yariv, Israel J. Chem., 7 (1969) 697.
40 S. Yariv, L. Heller and N. Kaufherr, Clays Clay Minerals, 17 (1969) 301.
41 L. Heller and S. Yariv, in: L. Heller (Ed.), Proc. Third Intern. Clay Conf., Tokyo 1969, Israel University Press, Jerusalem 1969, Vol. 1, p. 741.
42 L. Heller and S. Yariv, Israel J. Chem., 8 (1970) 391.
43 L. Heller-Kallai, S. Yariv and M. Riemer, Clay Minerals, 10 (1973) 35.
44 S. Yariv, Int. Rev. Phys. Chem., 11 (1992) 345.
45 S. Yariv and S. Shoval, Israel J. Chem., 22 (1982) 295.
46 Z. Yermiyahu, I. Lapides and S. Yariv, Clay Minerals, 38 (2003) 483.
47 S. Yariv, G. Kahr and A. Rub, Thermochim. Acta, 135 (1988) 299.
48 S. Yariv, M. Mueller-Vonmoos, G. Kahr and A. Rub, Thermochim. Acta, 148 (1989) 457.
49 S. Yariv, M. Mueller-Vonmoos, G. Kahr and A. Rub, J. Thermal Anal., 35 (1989) 1941.
50 S. Yariv, M. Mueller-Vonmoos, G. Kahr and A. Rub, J. Thermal Anal., 35 (1989) 1997.
51 S. Yariv, J. Thermal Anal., 36 (1990) 1953.
52 U. Shuali, S. Yariv, M. Steinberg, M. Mueller-Vonmoos, G. Kahr and A. Rub, Clay Minerals, 25 (1990) 107.
53 U. Shuali, S. Yariv, M. Steinberg, M. Mueller-Vonmoos, G. Kahr and A. Rub, Clay Minerals, 26 (1991) 497.
54 S. Yariv, in: W. Smykatz-Kloss and S. St. Warne (Eds) Lecture Notes in Earth Science 38. Thermal Analysis in the Geosciences, Springer Verlag, Berlin 1991, p. 328.
55 S. Yariv, in: R. Ikan (Ed.) Natural and Laboratory-Simulated Thermal Geochemical Processes, Kluwer Academic Pub., Dordrecht 2003, p. 253.
56 W. H. Allaway, Soil Sci. Soc. Amer. Proc., 13 (1949) 183.

57 W. F. Bradley and R. E. Grim, J. Phys. Chem., 52 (1948) 1404.
58 W. Bodenheimer, L. Heller and S. Yariv, Clay Minerals, 6 (1962) 167.
59 S. Yariv, Appl. Clay Sci., 24 (2004) 225.
60 S. Cebulak, A. Matuszewska and A. Langier-Kuźniarowa, J. Therm. Anal. Cal., 71 (2003) 905.
61 Z. Yermiyahu, A. Landau, A. Zaban, I. Lapides and S. Yariv, J. Therm. Anal. Cal., 72 (2003) 431.
62 N. Sonobe, T. Koyotani, Y. Hishiyama, M. Shiraishi and A. Tomita, J. Phys. Chem., 72 (1988) 7029.
63 N. Sonobe, T. Koyotani, Y. Tomita and A. Tomita, Carbon, 26 (1988) 573.
64 N. Sonobe, T. Koyotani, Y. Tomita and A. Tomita, Carbon, 28 (1990) 483.
65 N. Sonobe, T. Koyotani, Y. Tomita and A. Tomita, Carbon, 29 (1991) 61.
66 M. N. Bakola-Christianopoulopu, Polyhedron, 3 (1984) 729.
67 F. Feigl, Chemistry of Specific and Sensitive Reactions, Academic Press, New York 1949, p. 537.
68 M. Epstein, I. Lapides and S. Yariv, J. Therm. Anal. Cal., in press.
69 Z. Yermiyahu, I. Lapides and S. Yariv, Appl. Clay Sci., in press.
70 D. Garfinkel-Shweki and S. Yariv, Colloid Polym. Sci., 273 (1995) 453.
71 D. Garfinkel-Shweki and S. Yariv, J. Colloid Interface Sci., 188 (1997) 168.
72 D. Garfinkel-Shweki and S. Yariv, Clay Minerals, 32 (1997) 653.
73 D. Garfinkel-Shweki and S. Yariv, Clay Minerals, 34 (1999) 459.
74 R. Cohen and S. Yariv, J. Chem. Soc. Faraday Trans. 1, 80 (1984) 1705.
75 G. Rytwo and E. Ruiz-Hitzky, J. Therm. Anal. Cal., 71 (2003) 751.